Analyst

Accepted Manuscript

ROYAL SOCIETY OF CHEMISTRY

www.rsc.org/analyst

Contribution of rotational diffusivity towards the transport of antigens in heterogeneous immunosensors

Dharitri Rath[1,2] and Siddhartha Panda[1,2,3,*]

[1]Department of Chemical Engineering,

[2]Centre for Environmental Sciences and Engineering,

[3]Samtel Centre for Display Technologies,

Indian Institute of Technology Kanpur,

Kanpur - 208 016, UP, India

* Corresponding author

Tel: +91-512-259-6146

Fax: +91-512-259-0104

E-mail: spanda@iitk.ac.in

ABSTRACT

Higher capture efficiency in heterogeneous immunosensors is desirable for the detection of cancer biomarkers at low concentrations. The process of the capture of these antigens is transport limited since the rates of the antigen/antibody reactions are faster. In case of non-flow systems, the diffusive transport has contributions from both translational and rotational phenomena. Since the contribution of the rotational diffusivity is comparatively less explored in literature, we have studied the same for three antigens- bovine serum albumin (BSA), prostate specific antigen (PSA) and C-reactive proteins (CRP). We quantified the rotational diffusivities using the time resolved fluorescence anisotropy method, and further quantified the contribution of the rotational diffusivities to the overall diffusivity of the antigens, and also studied the effect of the process parameters- temperature and pH of the solution. With increase in temperature, the rotational diffusivity increased showing an Arrhenius dependency while with the variation of pH, it showed a non-monotonic behavior having maxima closer to the isoelectric point of the corresponding antigens. This interesting behavior of the pH values could be attributed to lesser electro-viscous effects when the antigen molecule is neutral around its isoelectric point. The optimization of the pH and temperature for the immunosensors could be utilized to design efficient immunosensors.

Keywords: Immunosensors; Fluorescence anisotropy; Rotational diffusivity; Antigens.

Nomenclature

C	Concentration of antigen in the solution at any time (mol/m^3)
D_{eff}	Effective diffusivity of the antigen in the solution (m^2/s)
D_{trans}	Translational diffusivity of the antigen in the solution (m^2/s)
D_{rot}	Rotational diffusivity of the antigen in solution (1/s)
D_{rot}'	Contribution of rotational diffusivity to D_{eff} (m^2/s)
$D_{0,rot}$	Pre-exponential factor in the Arrhenius dependency of D_{rot} (m^2/s)
$E_{a,rot}$	Activation energy for D_{rot} (KJ/mol)
G	G-factor for the sensitivity of the instrument
k_B	Boltzmann constant (J K^{-1})
r_1	Pre-exponential factor for the antigen
r_2	Pre-exponential factor for FITC
r	Fluorescence anisotropy of the antigen
r_h	Hydrodynamic radius (m)
R	Universal gas constant (J mol^{-1} K^{-1})
t	Time (s)
T	The absolute temperature (K)
v	Velocity of the antigen
η	Dynamic viscosity (N s/m^2)
θ	Rotational correlation time-constant for the antigen (s)
θ_1	Rotational correlation time-constant for FITC (s)

1. Introduction:

Heterogeneous immunosensors can provide specific and reliable detection of life threatening diseases like cancer in the early stages with the help of some signature proteins known as cancer biomarkers[1]. The investigations of physicochemical properties of these clinically relevant biomarkers are of great interest to the scientific community for improving the detection limit by enhancing their capture in an immunosensor[2]. The major challenge associated with the detection of these biomarkers is their extremely low concentration level in the human body. Hence, development of a fast, accurate, and efficient immunosensor is of great importance[3, 4]. The detection process in heterogeneous immunosensors includes two major events - the transport of analytes from the bulk to the surface, and the reaction of these analytes with the surface immobilized antibodies. Since the reaction kinetics of the antigen-antibody interaction is faster compared to the rate of transport of the analytes, the phenomena of the capture of analytes is transport limited[5]. Hence in order to design efficient immunosensors, alleviation of the transport limitations is crucial. Literature contains various reports, wherein efforts have been made to mitigate the mass-transfer limitations such as increasing the advective mixing by mechanical stirring[6, 7], thermal effects[8], AC electroosmosis[9], electrothermal effects[10, 11], and optimization of the pH[7, 12]. In non-flow systems, diffusion is the major mechanism of transport, and hence effective diffusivity (D_{eff}) is an important transport parameter, which combines the contributions from translational and rotational mobility of the travelling molecules. The effect of various process conditions on D_{eff} have been studied extensively; however the contribution of the rotational diffusivity towards the overall transport is comparatively less explored, and needs attention. We have tried to address this issue in the present study.

Rotational diffusion is a manifestation of the rotational degree of freedom of the analyte molecule which originates from the randomization of the orientations of the molecule, and is attributed to the nature of the interaction of the same with the surrounding medium (solvents as well as other solute molecules)[13]. There are studies reported in literature wherein the rotational dynamics of the molecules have been explored by various techniques for a variety of applications. The techniques used to measure rotational mobility of the molecules include phosphorescence anisotropy[14, 15], fluorescence anisotropy[16, 17], dynamic light scattering (DLS)[18, 19], nuclear magnetic resonance (NMR)[20], fluorescence correlation spectroscopy (FCS)[21] etc. Molecular dynamics simulation studies have also been used to calculate the rotational diffusivity[22, 23].

In time-resolved fluorescence anisotropy, the technique used in the present work to measure the rotational diffusivity of antigens, the rotational mobility of a fluorophore attached to the molecule is measured using a technique based on the time evolution of two polarized intensities to measure the fluorescence anisotropy decay[24], and is used to investigate the physical and chemical properties of these molecules. Since the rotational mobility strongly depends on the solute-solvent interactions as well as the structure of molecule, time-resolved fluorescence anisotropy measurement has been extensively used to capture the information associated with the dynamic nature and structural information of the molecules[25]. For example, Ao-Jin et al. estimated viscosity and the rotational diffusion of bacteriorhodopsin inside membranes to be used to monitor the oligomeric state of the membrane proteins, and showed the temperature dependencies of the viscosity values for the solvents under study[26]. Das et al. measured the rotational time constants of Coumarin-153 in pure 1-(2-methoxyethyl)-1-methylpyrrolidinium tris(pentafluoroethyl)trifluorophosphate (ionic liquid), and its mixture with toluene, and reported

that the rotational diffusion becomes faster in the presence of toluene[27]. Zheng et al. studied the dynamics of the decay of fluorescence anisotropy of free and bound NADH molecules in normal and cancerous tissues with the change in the environment of the endogenous fluorophore, which could be used to detect cancers at early stages[24]. Hu et al. reported the rotational time constant of T4 lysozyme and its dynamical nature pertinent to its physiological environment inside cells, which are pertinent to the applications in cell signaling[28]. Lavalette et al. reported the rotational Brownian motion of bovine serum albumin (BSA), hemoglobin and fragmented hemoglobin to check the validation of the Stokes-Einstein-Debye equation by changing the viscosity of the solution applied to quantify nonhomogeneity in-vivo[29]. Takahashi et al. studied the effect of various solvents on lysozyme-lysozyme interactions via fluorescence anisotropy measurements of the solution to quantify protein-protein interactions for various applications[30]. Further, anisotropy decay and change in the polarization of the fluorescence emission has also been used for detection purposes[31-33]. Though there are extensive studies on the quantification of the rotational time constant in various applications, to the best of our knowledge, the investigation of rotational time constants to quantify the contribution of rotational diffusion of molecules towards the overall diffusive transport for immunosensing applications have not been reported.

In the present study, we have investigated the effect of the major process parameters on the rotational diffusivity, which include temperature and pH of the solvent**.** While there are reports on the effect of temperature on D_{rot} for various molecules including bovine serum albumin (BSA)[34], the effect of temperature on D_{rot} for prostate specific antigen (PSA), and C-reactive proteins (CRP), and the effect of pH of the antigen solution, has not been explored till now. The motivation for the present study comes from our previous work, where we have optimized the pH of the solution to obtain the highest capture of the three antigens- BSA, PSA,

and CRP[7] for immunosensors. The pH values in the previous study were selected on the basis of the isoelectric points of the antigen and antibody molecules, and it was observed that maximum capture of the antigen molecules occurred at a pH value in between the pIs of the antigen and the antibody. Further, we obtained functional dependencies of transport and reaction parameters on three process parameters (temperature, extent of mixing and pH). A transport parameter analyzed for a non-flow system in our previous study through the kinetics of capture of the antigens was D_{eff}, hence it is of further interest to quantify the contribution of D_{rot} in the overall rate of transport, which was not studied in the previous work. We have measured the D_{rot} of the three FITC-tagged antigens - BSA, PSA, and CRP in the buffer solution by time-resolved fluorescence anisotropy method. Our goal is to quantify the contribution of rotational diffusivity to the overall diffusivity of the travelling molecule before reaching the electric double layer at the interface of surface immobilized antibodies and the electrolyte. So, the experiments were performed only in the buffer without any immobilized reacting surface. While BSA is chosen in order to benchmark our results, to the best of our knowledge, we could not find any report in the literature related to the measurement of rotational diffusivity of PSA and CRP. Anisotropy measurements were performed to obtain the rotational time constants, which were further used to calculate the contribution of D_{rot} for all three antigens. As the transport of analytes is the rate limiting step in most of the antigen-antibody interactions, the quantification of the contribution rotational diffusion towards the overall mass transport will be useful to design efficient microfluidic immunosensors for early disease detection[35].

2. Theory:

The mass transport of an analyte (the antigen molecules in the present study) is governed by a diffusion-convection phenomenon, described by equation 1.

$$\frac{\partial C}{\partial t} = \nabla.(D_{eff}\nabla C) - \nabla.(\vec{v}C) \quad (1)$$

The first term on the right hand side captures the effect of molecular diffusion on transport, whereas the second term incorporates contribution of convection. In non-flow systems, only the molecular diffusion term accounts for mass transport, hence effective diffusivity, D_{eff}, becomes an important transport parameter. As discussed above, it combines the contributions from both the translational and rotational degrees of freedom, and is given by equation 2 and 3 [36].

$$D_{eff} = D_{trans} + D'_{rot} \quad (2)$$

where

$$D'_{rot} = \frac{2}{3} r_h^2 D_{rot} \quad (3)$$

where the hydrodynamic radius of the molecules depends on the volume of the solute and their interaction with the surrounding solvent molecules.

Figure 1 shows the schematic to describe the process of the time-resolved anisotropy decay, and how it is utilized to extract the rotational time constants and the D_{rot}. As presented in the figure, the anisotropy measurements are based on the capture of the intensity of the emitted

light by fluorophores attached to the molecules having random orientations excited by linearly polarized light[37]. The orientation of the molecule plays a crucial role in the depolarization of the incoming light, and provides information about the rotational degrees of freedom of the molecule. Polarizers were used in the path of the emitted light to collect the parallel and perpendicular components of the depolarized emitted light recorded as a function of time. The collected data were processed by the spectrometer to obtain the anisotropy as a function of time. A multi-exponential fit to the anisotropy decay data was used to obtain the rotational time constant of various species present in the solution. For a fluorophore tagged antigen molecule, a bi-exponential function given by equation 4[30], was fitted to the anisotropy decay data.

$$r(t) = r_1 \exp(-t/\theta) + r_2 \exp(-t/\theta_1) \quad (4)$$

Assuming the antigen molecules to be spherical in shape (Stoke's approximation), the rotational correlation time constant obtained from the exponential decay fit can be used to calculate the rotational diffusion coefficient by equation 5[38].

$$D_{rot} = \frac{1}{6\theta} \quad (5)$$

The hydrodynamic radius (r_h) was calculated from D_{rot} by equation 6[38].

$$r_h = \left(\frac{k_B T}{8\pi\eta D_{rot}} \right)^{1/3} \quad (6)$$

The above expression is obtained from the Stokes-Einstein Debye relation, which incorporates the change in volume due to the change in the environment in which the antigen molecules are kept.

3. Materials and methods:

3.1 Chemicals:

Phosphate buffer saline (PBS) of pH 7.4 was obtained from Sigma-Aldrich Inc. Other buffer solutions of pH 4, 5, 6, 6.5 and 8 were prepared taking appropriate combinations of sodium dihydrogen phosphate and monosodium phosphate salts, and the final pH was verified using a calibrated pH meter. The antigens were stored in a stock solution of standard PBS buffer of pH 7.4, and 10 µl of this stock solution was mixed with 2 ml of the buffer solution of the specific pH of interest. Furthermore, the final pH of the combination was measured to be the same (within the limits of accuracy of the instrument) as earlier. Bovine serum albumin (BSA) was obtained from Genei Biotech, Bangalore, India. Prostate specific antigen (PSA) was obtained from Fitzgerald Industries International, USA, and C-reactive proteins (CRP) from Calbiochem, USA. The tagging of the antigens (BSA, PSA and CRP) with fluorescein isothiocyanate (FITC) was accomplished in Genetech Laboratory, Biotech. Park, Lucknow, India, and the ratio of the FITC to antigen was assumed to be 1:1 (based on the manufacturer's information). The different dilutions for measurement were prepared using stock solutions of the above tagged antigens in the required buffer solution.

3.2 Process conditions used for experiments:

Three different antigens (BSA, PSA and CRP), at three different temperatures (293, 303, and 313 K) were used in the experiments. The antigen solution was added to the buffer of the required pH value, mixed well, and then poured into a clean cuvette for taking measurements. The pH values chosen for each of the antigen molecule on the basis of their isoelectric points, are listed in Table 1. Four/five values of pH, lower as well as higher than the pIs of the corresponding antigens, were used in the experiments.

Table 1. pH values used for measurement for BSA, PSA, and CRP.

Antigens used	pI [7]	pH values used
BSA	4.8	4, 5, 6 and 7.4
PSA	6.8	5, 6, 6.5 and 7.4
CRP	7.2	5, 6, 6.5, 7.4 and 8

3.3 Time-resolved anisotropy measurement:

The time-dependent fluorescence anisotropy measurements were performed using a LifeSpec-II luminescence spectrometer (Edinburgh Instruments, Ltd). A pico-second pulsed diode laser of 445 nm was employed as the excitation source, with the emission being recorded at 530 nm. A filter of 500 nm was used in the path of emitted light. Experiments were conducted in triplicates

for each process condition mentioned above, and the error bars represent one standard deviation about the mean.

3.4 Viscosity measurements:

The viscosity of the buffer solutions was measured using a Rolling-ball viscometer (Lovis 2000M Anton Paar microviscometer) at three temperatures (293, 303 and 313 K), where the pH was kept constant at 7.4. Further the viscosity measurements were taken at pH values of 4,5,6,6.5, and 7.4, with the temperature being kept constant at 303 K.

4. Results and Discussions:

The values of D_{rot} are expected to be dependent on various parameters associated with a solvent (viscosity, temperature, pH). So, we have studied the effect of the temperature, and the pH of the solution on D_{rot}, and further investigated the choice of the best process condition. Since the values of viscosity may vary with temperature, and pH of the solution, these were measured for each experimental condition used, and are reported in Table 2. We first used BSA to benchmark our results, and then conducted the rotational diffusion measurements of PSA and CRP.

Table 2. Viscosity values of the buffer measured at (a) three temperatures at pH 7.4, and (b) five pH values at 303 K.

(a)

***T* (K)**	**η (Pa.s) x 10^{-3}**
293	1.031
303	0.826
313	0.693

(b)

pH	**η (Pa.s) x 10^{-3}**
4	0.851
5	0.839
6	0.904
6.5	0.904
7.4	0.826
8	0.909

4.1 Temperature dependency and validation:

Fig. 2 shows the decay of the fluorescence anisotropy with time for BSA tagged with FITC, using PBS as the solvent at 303 K and pH 7.4. The anisotropy as a function of time thus obtained was fitted to a bi-exponential decay function, as shown by the solid line in the figure. The fitting yields the rotational correlation time constants associated with the tagged antigens. Similar anisotropy curves were obtained for BSA at 293 and 313 K, and also for PSA and CRP at all three temperatures, and for all three antigens at the pH values mentioned in Table 1. The

corresponding time constants obtained via fitting were used in calculating D_{rot} and r_h for each process condition using equations 4 and 5, respectively.

Fig. 3a shows the plot of D_{rot} of BSA molecules at pH 7.4 and three temperatures- 293, 303, and 313 K. We observed that for all cases, the values of D_{rot} increases with increase in temperature. The increase in D_{rot} with increase in temperature can be attributed to increased average kinetic energy of the molecules at higher temperature, which manifests in enhancement of both rotational and translational degrees of freedom. The above trends are also in accordance with the studies reported earlier. For example, increased rotational diffusivity values for bacteriorhodopsin with temperature were observed based on faster anisotropy decay, measured with the help of anisotropy measurements[26]. Temperature dependent studies have also been performed for 4-methyl-4'-cynanobiphenyl (1CB) and 4-hexyl-4'-cynanobiphenyl (6CB), and the time constants for the decay were reported to decrease with increase in temperature indicating increased values of D_{rot} with temperature[39].

Similar experiments were conducted for PSA and CRP as a function of temperature, and the results are plotted in Fig. 3b and c respectively. As expected, for all cases, D_{rot} increases with increase in temperature and showing an Arrhenius dependency, given by equation 7.

$$D_{rot} = D_{0,rot} \exp\left(-E_{a,rot}/RT\right) \qquad (7)$$

For the Arrhenius fitting shown in the insets of Fig. 3, the mean value of each case was taken into account, where R^2 represents the regression coefficient, and is used to show how well the experimental data is fitted to the Arrhenius model. After fitting D_{rot} vs. *temperature*, we obtained the values of $D_{0,rot}$ and $E_{a,rot}$ for BSA, PSA and CRP respectively, shown in Table 3. The

quantification of the dependencies of D_{rot} with temperature would be useful in selecting the temperature range for the respective antigen solution. Arrhenius dependencies of the rotational motion was earlier reported for BSA, with an activation energy of 13 KJ/mol[34]. The difference with our results could be due to the different experimental conditions used. To the best of our knowledge, such quantification for PSA and CRP have not been reported in the literature so far. After obtaining the data for the temperature dependencies of D_{rot} for the three antigens, we proceed to obtain the pH dependencies.

Table 3. Fitting parameters obtained from D_{rot} vs. T for all three antigens.

Antigen	$D_{0,rot}$ (1/s)	$E_{a,rot}$ (KJ/mol)	R^2
BSA	8.90×10^6	36.08	0.99
PSA	2.16×10^6	32.40	0.95
CRP	7.76×10^4	18.74	0.93

4.2 Effect of pH:

Fig. 4a shows the plot of D_{rot} at 303 K, and four different pH values of the solution for BSA. It can be observed from the figure that the D_{rot} shows maxima at pH 5, which is close to the isoelectric point of BSA having a value of 4.8[40]. Similarly Fig. 4b and c show the plots of the D_{rot} at 303 K, and four different pH values for PSA, and five different pH values for CRP respectively. It was observed that the maxima in both the cases are at about pH values of 6.5 and 7.4, close to their pIs at 6.8 and 7.2 respectively[7]. The occurrence of maxima of D_{rot} close to the

pI of the antigens can be attributed to minimal surface charge on the antigen molecules at this pH, which leads to weakening of the electrostatic interactions of the antigens with the surrounding (which includes other similar molecules as well as molecules of the solvent). However, at a pH away from the isoelectric point, the net surface charge of the molecules is either positive or negative which facilitates the electrostatic interactions of the molecules with other similar molecules and electrolyte carrier molecules (solvent molecules). This leads to electro-viscous effects that ultimately result in hindrance to the motion of the antigen molecules. Since the rotational mobility originates from the Brownian diffusivity of particles, we hypothesize that the electro-viscous effects result in lower values of D_{rot}. There are reports of similar observations to support our hypothesis. For example, Nesmelova et al. reported that protein molecules do not form aggregates due to absence of interaction at pH values where they have very small amount of surface charge, and hence leading to enhanced Brownian motion[41]. Tawari et al. studied Brownian diffusivity of Laponite clay particle in association with the electric double layer of the solute molecules[42], and reported that the charged disks have 50% smaller diffusivity than that of hard disks (no double layer) with the same diameter. They explained it in terms of electro-viscous drag offered to a charged solute particle by the surrounding cloud of the counter ions. Hence, we conclude that the maximum rotational mobility at the isoelectric point can be attributed to the least hindrance pertaining to low surface charge on the antigen molecules.

The above observations associated with pH variation suggest that at the pI of the antigen molecules, the maximum diffusivity is expected to result in the higher rate of transport, and hence higher capture of the analytes in the immunosensor. However, it is to be noted that the capture strongly depends on the affinity of two binding species along with the rate of transport of

antigens. Since opposite charges on the binding species enhances the probability of binding, one has to maintain a pH different from the pI values of both the species to get the maximum capture. These results seems to indicate that there is tradeoff between maximizing the rate of transport rate and the rate of capture of the antigens. However, in case of the immunosensors since one of the binding species (antibodies) is already immobilized on the reacting surface, the incoming antigen has to travel through the solvent onto the surface for the reaction to happen. Hence, a higher rate of transport may play a crucial role here. To make the above point more clear we discuss the present work in the context of our previous work. In our previous work, we had observed the maximum capture efficiency at a value of pH in between the isoelectric points (pI) of antigen and antibody[7], where our goal was to maximize the amount of the bound complex. So, we had studied the interaction between the incoming antigen and the immobilized antibody surface, and obtained maximum capture where the antigens and antibodies have opposite charges induced on their surfaces, which leads to the maximum electromigration when the antigen comes into the electrical double layer (EDL) associated with the immobilized antibody. However, before coming into the EDL, the antigens have to travel through the bulk solution where the various solvent conditions affect the motion of the antigen molecules, which could affect the transport. Thus while the maxima of the capture of antigens as a function of pH of the solution for the previous investigation was focused within the EDL of immobilized layer (i.e., closer to the surface), the maxima of the D_{rot} reported in the present work is pertinent when the antigens are outside EDL of the immobilized antibodies, and traveling through the solvent in the bulk layer. So, all the measurements are taken in the buffer solution for this work to quantify the diffusivity of the antigen molecules. As the effective diffusivity is contributed by the two degrees of freedom: translational and rotational, the individual contributions are expected to be higher at

this pH value. To the best of our knowledge, pH dependent studies for the three antigens are not reported in the literature. However, there are reports on the comprehensive studies of the interactions of different kinds of ionic liquids and their interactions with non-polar, charged and dipolar solute molecules and the factors that influence their anisotropy behavior[43]. Since, this interaction is specific to the solute-solvent pair under consideration, there is no unanimity in the trends obtained for the kind of interactions. For example, the rotational dynamics of a cationic solute ethidium bromide (EB) and an anionic solute 1-anilinonaphthalene-8-sulfonate (ANS), did not show any electrostatic interactions in ionic liquids[17]. On the contrary, the rotational diffusion of a cationic solute Rhodamine 110 in a mixture of solvents including SDS showed the dependence of the rotational time constants on the solute-solvent electrostatic interactions[16]. There are also reports of the study of neutral versus charged solutes in ionic liquids, but the charge components of the solute-solvent interaction were not quantified for the rotational dynamics[44].

4.3 Contribution to the effective diffusivity (D_{eff}):

From the experimentally measured time constants for all three antigens, and the process conditions such as temperature and pH of the solution, the values of τ and D_{rot} were obtained for each case. The D_{rot} was used to calculate r_h, and further D_{rot}' was calculated which quantifies the contribution of rotational diffusivity of molecule towards over all transport. Fig. 5a shows the plot of D_{rot}' for BSA as a function of temperature and pH. It is observed that the factor D_{rot}' increases monotonically with temperature in the range studied, while it shows a maxima with the pH of the solution. These trends observed here resemble that of the observed values for D_{rot}

reported in Fig. 3 and 4, though the absolute values are different for each case. Similar data were plotted for PSA and CRP as a function of temperature and pH in Fig. 5b and c respectively. The increment in the values of D_{rot}' with temperature follows a similar Arrhenius dependency for both PSA and CRP in the ranges studied whereas a nonmonotonic behavior is observed with the variation in pH values. However, the variation in D_{rot}' with pH for CRP, reported in Fig. 5c shows a maxima at pH 7.4 which is close to pI of CRP while the other data points are within the statistical limits of error. The values of D_{rot}' were found to be in the range of the values of D_{eff} (1 x 10^{-9} to 1 x 10^{-12} m^2/s) reported earlier[2, 45].

5. Conclusions:

Rotational diffusivity is an important transport parameter and needs to be characterized to help design an efficient immunosensor. In this work, the D_{rot} is measured for three antigens- BSA, PSA and CRP in the buffer, using the technique of time-resolved fluorescence anisotropy. Further, the effects of two important process parameters (temperature and pH) on the values of D_{rot} were investigated. The values of D_{rot} increase with temperature showing Arrhenius dependencies which were quantified through the fitting parameters. The trend with the variation in pH shows an interesting behavior - a maxima at a pH close to the isoelectric point of the corresponding antigens. This is attributed to the lesser hindrance due to lesser electro-viscous effects, leading to higher values of D_{rot} when the antigen molecules are neutral as compared to the cases when they are either positively or negatively charged. Furthermore, the contribution of D_{rot} (given by D_{rot}') was quantified, and it was found to be of the order of 1 x 10^{-11} m^2/s, which also measures the contribution towards the diffusive transport of the antigens in an

immunosensor. In this work, we have obtained D_{rot} through anisotropy measurements for PSA and CRP, which we believe is reported for the first time. Further, the quantification of D_{rot} for the antigens with variation in the process parameters (temperature and pH) was studied. Delineating the contributions of each of the parameters in the diffusive transport processes involved would help optimize the transport parameters for immunosensors.

Acknowledgement

The authors gratefully acknowledge the financial support from the DST Science and Engineering Research Board, India (Grant No. SB/S3/CE/055/2013). Kind support for measurement of fluorescence anisotropy by Ms. B. Sengupta and Prof. P. Sen in the Department of Chemistry, IIT Kanpur, is acknowledged.

References:

1. V. Kulasingam and E. P. Diamandis, *Nat. Rev. Clin. Oncol.*, 2008, **5**, 588-599.
2. D. Rath, S. Kumar and S. Panda, *Mater. Sci. Eng., C*, 2012, **32**, 2223-2229.
3. A. Bange, H. B. Halsall and W. R. Heineman, *Biosens. Bioelectron.*, 2005, **20**, 2488-2503.
4. R. Chepyala and S. Panda, *Appl. Surf. Sci.*, 2013, **271**, 77-85.
5. T. M. Squires, R. J. Messinger and S. R. Manalis, *Nat. Biotech.*, 2008, **26**, 417-426.
6. G. Wang, J. D. Driskell, M. D. Porter and R. J. Lipert, *Anal. Chem.*, 2009, **81**, 6175–6185.
7. D. Rath and S. Panda, *Chem. Eng. J.*, 2015, **260**, 657-670.

8. H. S. Fogler, *Elements of Chemical Reaction Engineering*, fourth edn., Prentice Hall International series, 2005.

9. R. Harta, R. Leca and H. M. Noh, *Sens. Actuators, B*, 2010, **147**, 366–375.

10. M. Sigurdson, D. Wamg and C. D. Meinhart, *Lab Chip*, 2005, **5**, 1366–1373.

11. K. R. Huang, J. S. Chang, S. D. Chao, K. C. Wu, C. K. Yang, C. Y. Lai and S. H. Chen, *J. Appl. Phys.*, 2008, **6**, 064702–064711.

12. N. Gan, L. Jia and L. Zheng, *Int. J. Mol. Sci.*, 2011, **12**, 7410–7423

13. M. A. Charsooghi, E. A. Akhlaghi, S. Tavaddod and H. R. Khalesifard, *Comput. Phys. Commun.*, 2011, **182**, 400-408.

14. G. H. Koenderink, D. G. A. L. Aarts and A. P. Philipse, *J. Chem. Phys*, 2003, **119**, 4490-4499.

15. G. H. Koenderink, M. P. Lettinga and A. P. Philipse, *J. Chem. Phy.*, 2002, **117**, 7751-7764.

16. K. S. Mali, G. B. Dutt and T. Mukherjee, *J. Phys. Chem. B*, 2007, **111**, 5878-5884.

17. D. C. Khara and A. Samanta, *Phys. Chem. Chem. Phys.*, 2010, **12**, 7671-7677.

18. R. Piazza and V. Degiorgio, *J. Phys.: Condens. Matter*, 1996, **8**, 9497–9502.

19. R. Pecora, *J. Nanopart. Res.*, 2000, **2**, 123–131.

20. S. Ravindranathana, C. H. Kimb and G. Bodenhausen, *J. Biomol. NMR*, 2005, **33**, 163–174.

21. A. Loman, I. Gregor, C. Stutz, M. Mund and J. Enderlein, *Photochem. Photobiol.*, 2010, **9**, 627-636.

22. G. F. Schroder, U. Alexiev and H. Grubmuller, *Biophys. J.*, 2005, **89**, 3757–3770.

23. V. Wong and D. A. Case, *J. Phys. Chem. B*, 2008, **112**, 6013-6024.

24. W. Zheng, D. Li and J. Y. Qu, *J. Biomed. Opt.*, 2010, **15**, 037013.

25. M. Ameloot, M. VandeVen, A. U. Acuna and B. Valeur, *Pure Appl. Chem.*, 2013, **85**, 589–608.

26. W. Ao-Jin and H. Kun-Sheng, *Chin. Phys. Lett.*, 2002, **19**, 1727-1729.

27. S. K. Das and M. Sarkar, *J. Mol. Liq.*, 2012, **165**, 38-43.

28. D. Hu and H. P. Lu, *J. Phys. Chem. B*, 2002, **107**, 618-626.

29. D. Lavalette, C. Tetreau, M. Tourbez and Y. Blouquit, *Biophys. J.*, 1999, **76**, 2744-2751.

30. D. Takahashi, E. Nishimoto, T. Murase and S. Yamashita, *Biophys. J.*, 2008, **94**, 4484-4492.

31. A. P. Demchenko, *Introduction to Fluorescence Sensing*, Springer Science & Business Media B.V. , 2009.

32. S. J. Zhen, Y. Yu, C. M. Li and C. Z. Huang, *Analyst*, 2015, **140**, 353-357.

33. W. Li, K. Wang, W. Tan, C. Ma and X. Yang, *Analyst*, 2007, **132**, 107-113.

34. M. L. Ferrer, R. Duchowicz, B. Carrasco, J. de la Torre and A. U. Acuna, *Biophys. J.*, 2001, **80**, 2422-2430.

35. R. Chepyala and S. Panda, *Microfluid. Nanofluid.*, 2015, **DOI 10.1007/s10404-014-1532-6**, 1-11.

36. G. Gros, D. Lavalette, W. Moll, H. Gros, B. Amand and F. Pochon, *Proc. Natl. Acad. Sci.*, 1984, **81**, 1710-1714.

37. J. R. Lakowicz, *Principles of Fluorescence Spectroscopy*, Third edn., Springer Science & Business Media, 2007.

38. Y. Y. Kuttner, N. Kozer, E. Segal, G. Schreiber and G. Haran, *J. Am. Chem. Soc.*, 2005, **127**, 15138-15144.

39. H. Matsuzawa, K. Watanabe and M. Iwahashi, *J. Oleo Sci.*, 2007, **56**, 579-586.

40. C. Wang, J. Wang and L. Deng, *Nanoscale Res. Lett.*, 2011, **6**, 579.

41. I. V. Nesmelova, V. D. Skirda and V. D. Fedotov, *Biopolymers*, 2002, **63**, 132-140.

42. S. L. Tawari, D. L. Koch and C. Cohen, *J. Colloid Interface Sci.*, 2001, **240**, 54-66.

43. K. S. Mali, *J. Chem. Sci.*, 2009, **121**, 7-21.

44. N. Ito, S. Arzhantsev and M. Maroncelli, *Chem. Phys. Lett.*, 2004, **396**, 83-91.

45. R. A. Vijayendran, F. S. Ligler and D. E. Leckband, *Anal. Chem.*, 1999, **l71**, 5405-5412.

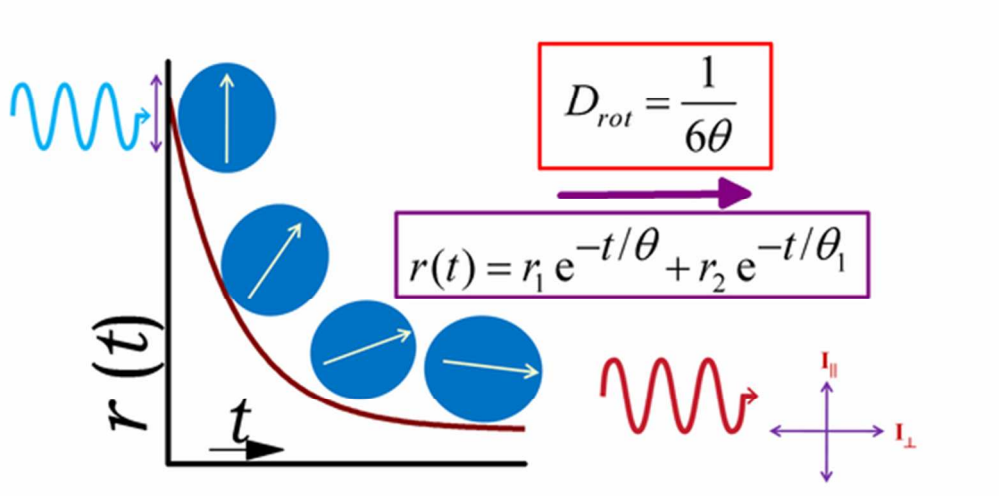

Figure 1
49x24mm (300 x 300 DPI)

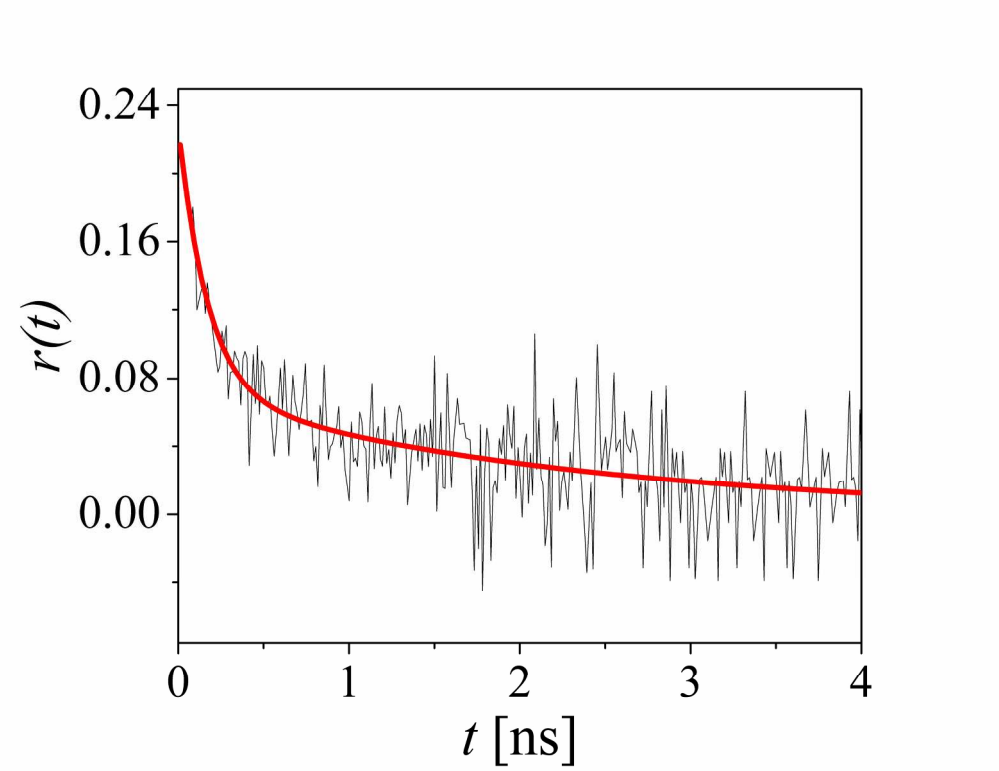

Figure 2
215x166mm (300 x 300 DPI)

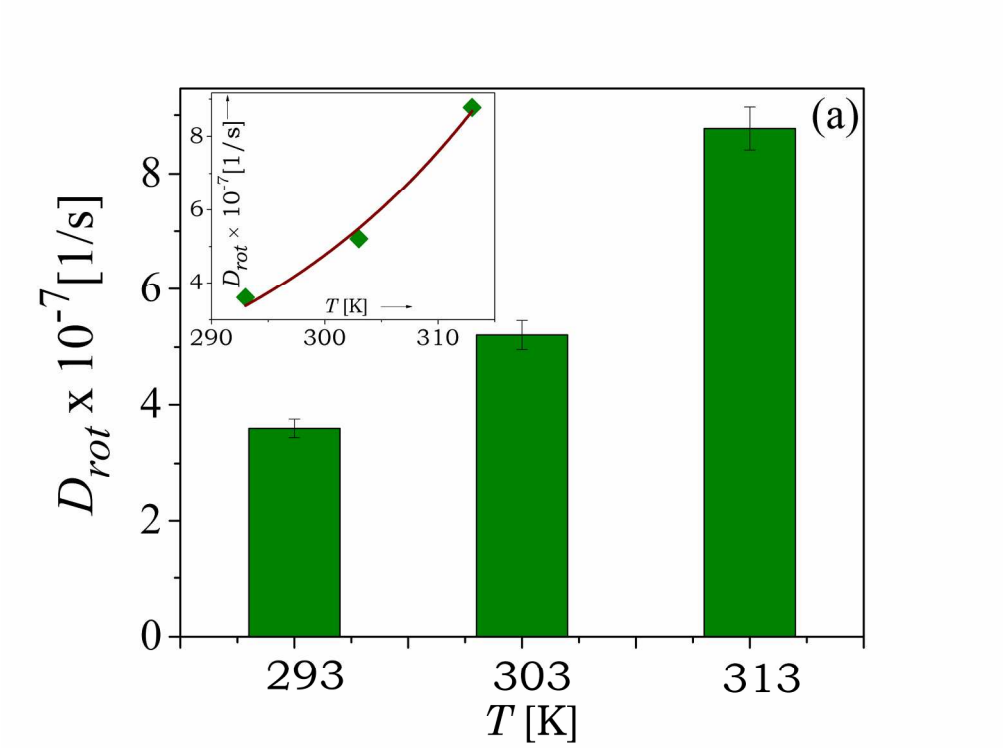

Figure 3
207x158mm (300 x 300 DPI)

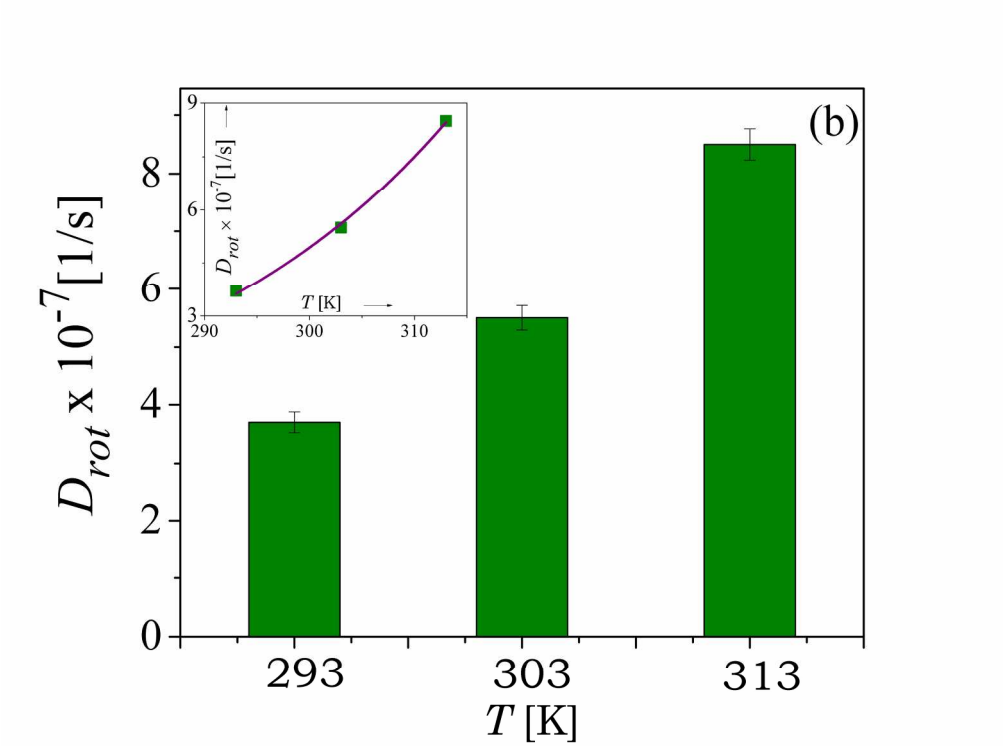

Figure 3b
207x158mm (300 x 300 DPI)

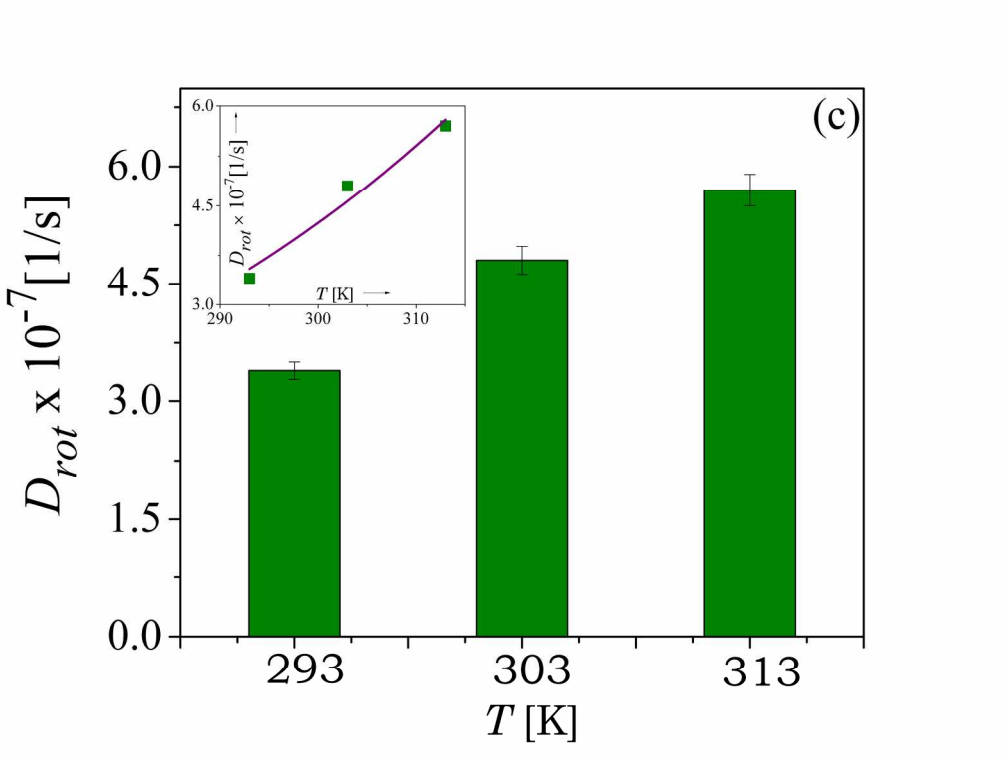

Figure 3c
207x158mm (300 x 300 DPI)

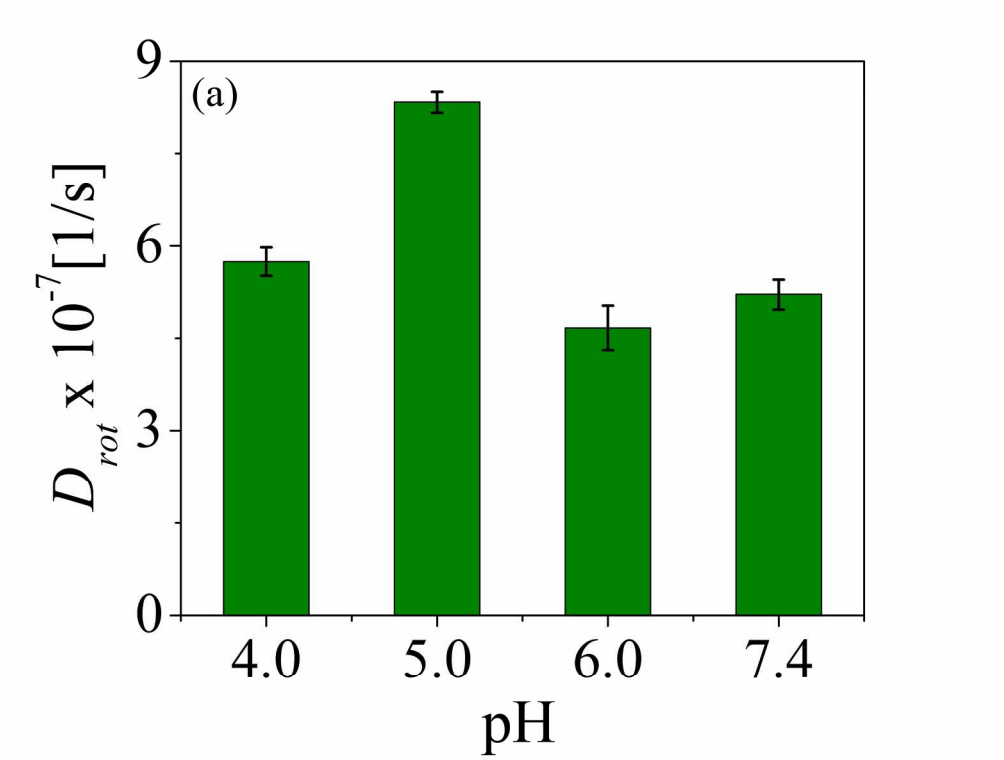

215x166mm (300 x 300 DPI)

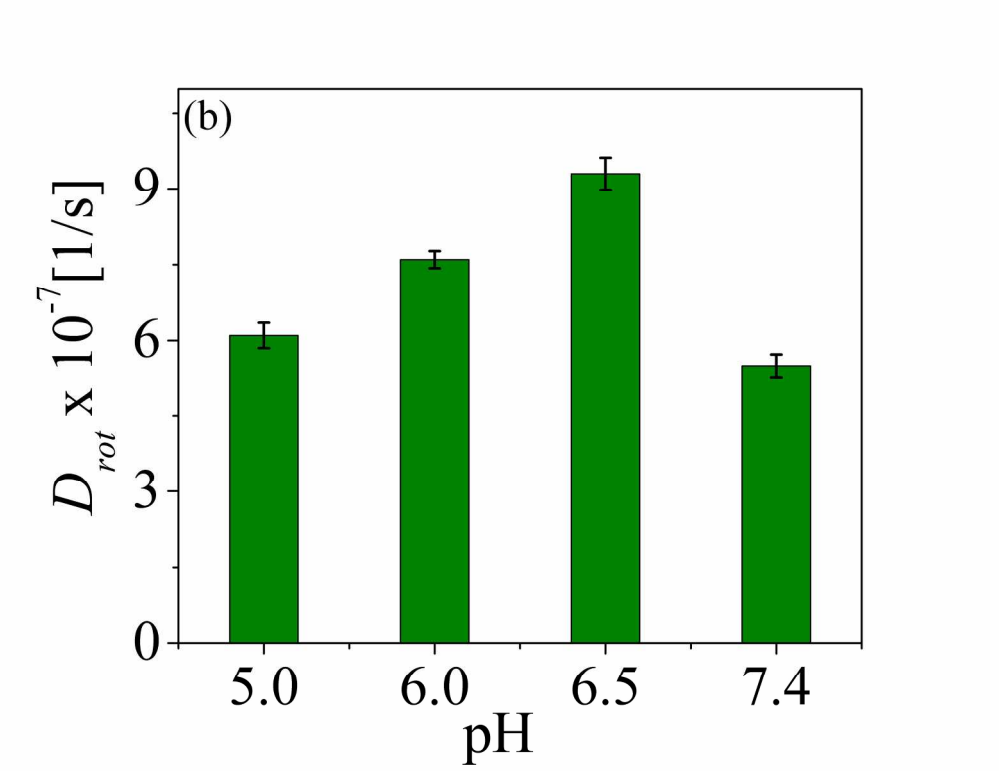

215x166mm (300 x 300 DPI)

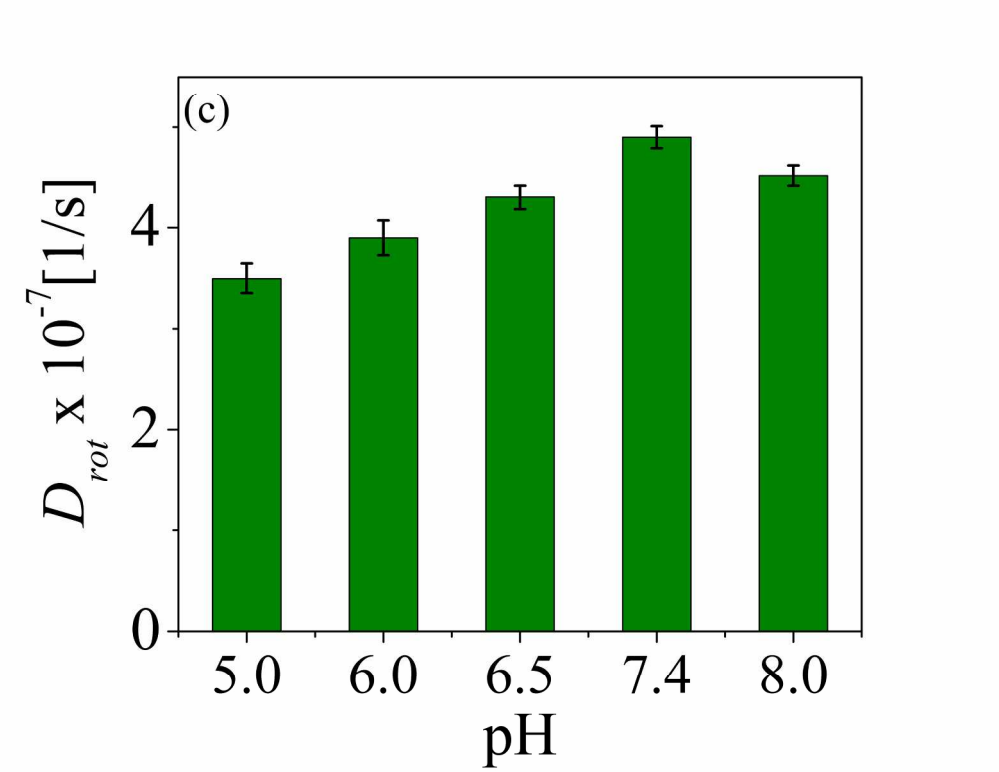

215x166mm (300 x 300 DPI)

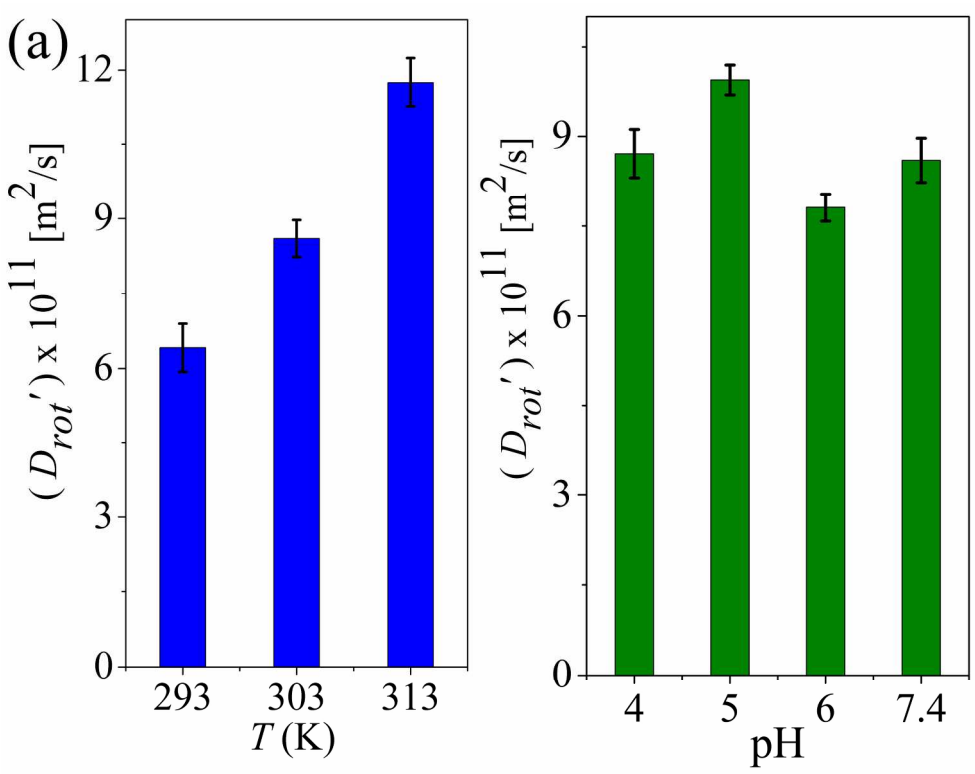

215x166mm (300 x 300 DPI)

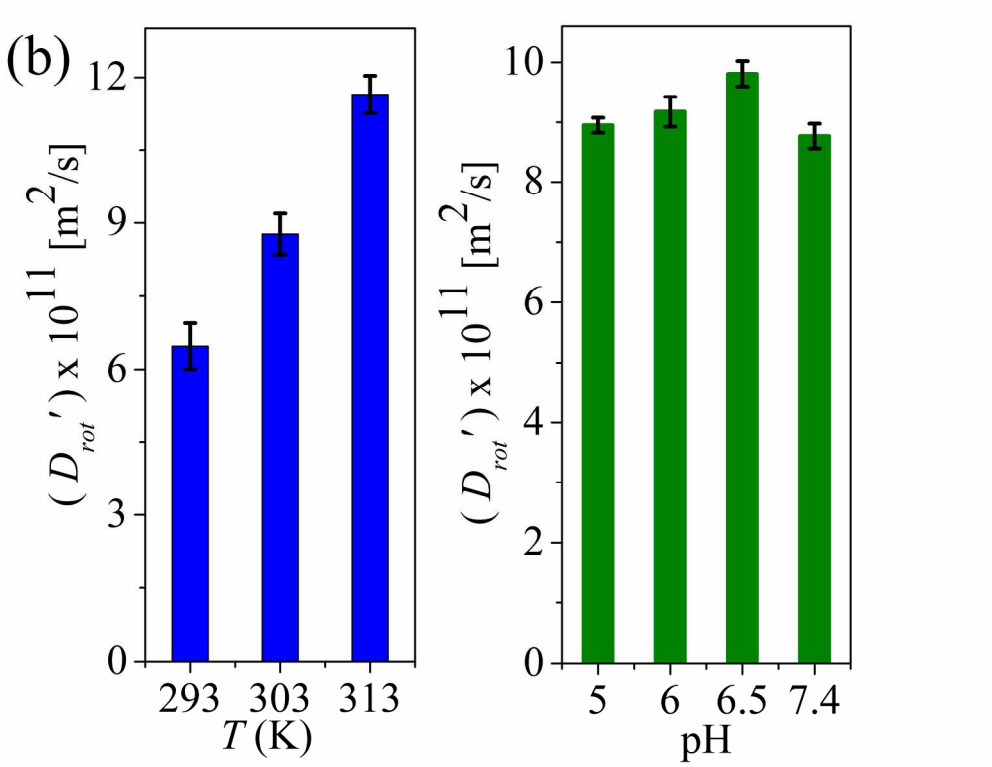

215x166mm (300 x 300 DPI)

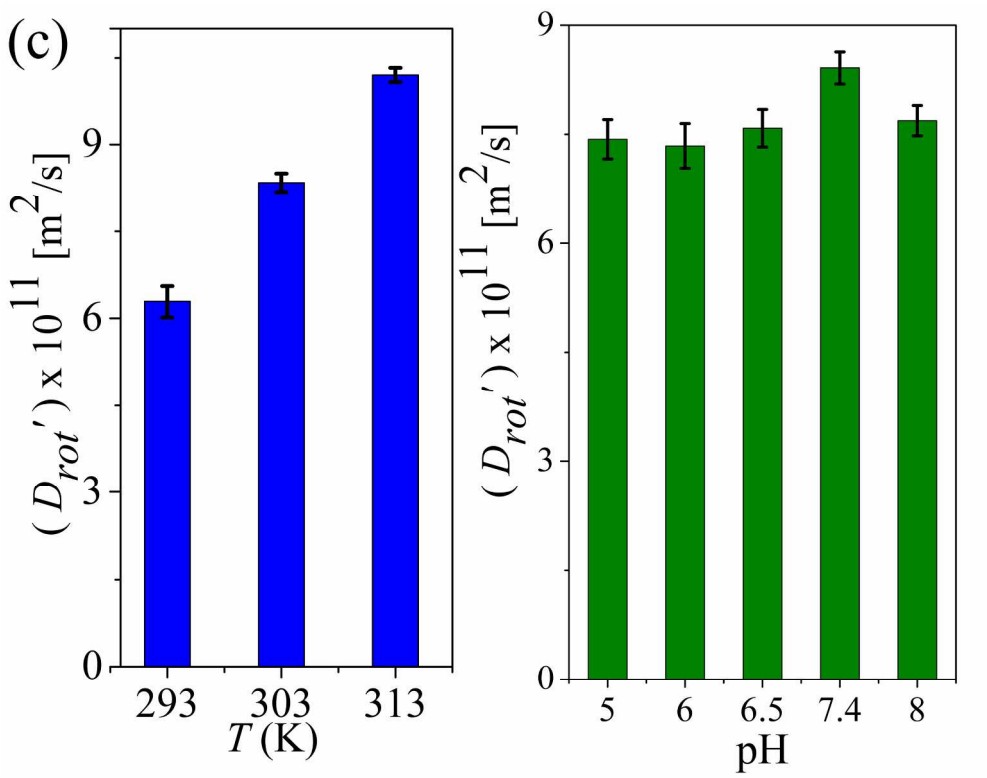

215x166mm (300 x 300 DPI)

List of Tables:

1. pH values used for measurement for BSA, PSA, and CRP
2. Viscosity values of the buffer measured at (a) three temperatures at pH 7.4, and (b) five pH values at 303 K.
3. Fitting parameters obtained from D_{rot} vs. T for all three antigens

List of Figures:

1. Schematics representing the overall process of the time-resolved anisotropy decay.
2. Time-resolved anisotropy decay curve for BSA at 30 ^{o}C and pH 7.4. The solid line represents the bi-exponential fit to the experimental anisotropy decay data.
3. The values D_{rot} at pH 7.4 and three temperatures- 293, 303 and 313 K, and the corresponding Arrhenius fitting is presented in the inset for (a) BSA (b) PSA and (c) CRP.
4. The values D_{rot} as a function of pH at T= 303 K for (a) BSA, (b) PSA, and (c) CRP.
5. The values of D_{rot}' as a function of temperature (keeping pH constant at 7.4), and pH (keeping temperature constant at 303 K) for (a) BSA, (b) PSA, and (c) CRP.